1 Introduction to Different PET Radiopharmaceuticals and Hybrid Modalities (PET/CT and PET/MRI)

Luca Giovanella, Lisa Milan, and Arnoldo Piccardo

1.1 Physical Principles of Positron Emission Tomography and Hybrid Modalities

Positron Emission Tomography (PET) is an imaging technique performed by using positron emitting radiotracers. Positron decay occurs with neutron-poor radionuclides and consists in the conversion of a proton into a neutron with the simultaneous emission of a positron (β+) and a neutrino (ν). The positron has a very short lifetime, and after the annihilation with an electron simultaneously produces two high-energy photons (E = 511 keV) in approximately opposite directions that are detected by an imaging camera. The PET scanning is based on the so-called annihilation coincidence detection (ACD) of the 511 keV γ-rays after the annihilation. Tomographic images are formed collecting data from many angles around the patient by scintillating crystals optically coupled to a photon detectors used to localize the position of the interaction and the amount of absorbed energy in the crystals (Table 1.1) [1].

Table 1.1 Properties of PET scintillator crystals

	NaI(Tl)	BGO	LSO	GSO	LYSO
Effective atomic number (Z)	50	73	66	59	60
μ (cm^{-1})	0.34	0.95	0.87	0.70	0.86
Index of refraction	1.85	2.15	1.82	1.85	1.81
Density (g/cm^3)	3.67	7.13	7.40	6.71	7.30
Photon yield (per kVp)	38	8	20–30	12–15	25
Peak wavelength (nm)	410	480	420	430	420
Decay time constant (ns)	230	300	40	65	41
Energy resolution (% at 511 keV)	7.8%	20%	10.1%	9.5%	20%
Hygroscopic	Yes	No	No	No	No

L. Giovanella (✉)
Clinic of Nuclear Medicine and Molecular Imaging, Imaging Institute of Southern Switzerland, Ente Ospedaliero Cantonale, Bellinzona, Switzerland

Laboratory of Radiomics and Predictive Imaging, Imaging Institute of Southern Switzerland, Ente Ospedaliero Cantonale, Bellinzona, Switzerland

Clinic of Nuclear Medicine, University Hospital and University of Zurich, Zurich, Switzerland
e-mail: luca.giovanella@eoc.ch

L. Milan
Clinic of Nuclear Medicine and Molecular Imaging, Imaging Institute of Southern Switzerland, Ente Ospedaliero Cantonale, Bellinzona, Switzerland

Laboratory of Radiomics and Predictive Imaging, Imaging Institute of Southern Switzerland, Ente Ospedaliero Cantonale, Bellinzona, Switzerland

A. Piccardo
Division of Nuclear Medicine, Ente Ospedaliero "Ospedali Galliera", Genoa, Italy

G. Treglia, L. Giovanella (eds.), *Evidence-based Positron Emission Tomography*,
https://doi.org/10.1007/978-3-030-47701-1_1

Table 1.2 The PET scanner performance and the intrinsic PET limitations

	Definition	Intrinsic limitation
Spatial resolution	The minimum distance between two points in an image that can be detected by a scanner	*Positron range*: Error occurs in the localization of the true position of the positron emission resulting in the degradation of the spatial resolution *Non-collinearity*: The two 511 keV photons are not emitted at exactly opposite directions: This deviation can reach a value of ±0.25° at maximum *detector size and its intrinsic resolution:* resolution is better in the centre of the FOV than at the edge
Sensitivity	Number of counts per unit time detected by the system for a unitary activity	*Geometric efficiency*: the fraction of emitted radiation that hits the detector and it depends on the source to detector distance, on the diameter of the ring and on the number of detectors in each ring *Intrinsic efficiency*: the fraction of radiation that reaches the detector and is acquired. It depends on the scintillation decay time and the stopping power of the detector
Noise-equivalent count rate	Parameter used to define the noise and to compare the PET performance	Takes into account the effects introduced by scatter and random coincidences
Contrast	Difference in counts between an area of interest and its surroundings	Scatter, random and out-of-FOV radiation

The key properties that characterize the PET scanner performances are the spatial resolution, the sensitivity, the Noise-Equivalent Count Rate (NECR) and the contrast [2]. The projection data acquired in the form of sinograms are affected by a number of factors that contribute to the degradation of the final images and hence to the PET scanner performances, as reported in Table 1.2.

Two classes of reconstruction techniques exist: the analytical and the iterative methods [3]. The most used analytical method is the backprojection. To compensate the blurring, a filter is applied to the projections before they are back-projected onto the image [i.e. filtered backprojection (FBP)]. In modern scanners, the image reconstruction algorithms are based on iterative methods, which approach the true image by means of successive estimations, in order to converge to an image that best represents the original object. These algorithms are known as expectation maximization (EM) and Ordered Subset Expectation Maximization (OSEM) algorithm [4].

1.2 Hybrid Scanners: PET/CT and PET/MRI

Combined PET/CT systems were commercially available from 2001 and in a very short time the dedicated PET scanner was completely replaced by hybrid PET/CT. The ability of hybrid PET/CT systems to accurately identify the anatomic location of diseases and to provide attenuation-corrected images are the main causes of their rapid success and diffusion [5]. Modern clinical PET/CT consists in a high-performance PET scanner in-line with a high-performance CT scanner arranged in sequential gantries. The scanner table moves along the gantry axis in order to subsequently acquire CT and then PET data. A software integrated in the system has to check if the patient bed undergoes some deflections during the translation [6]. Images of tissue attenuation from the CT scan are used to derive the PET attenuation correction factors. The latter depends on the energy of the photons: since CT X-rays and PET γ-rays have an energy of 70 keV and 511 keV,

Table 1.3 The characteristics of the three commercially available PET/MRI scanners

	Siemens biograph mMR	Philips ingenuity	GE Signa
PET/MR technology	Integrated	Sequential	Integrated
PET			
Scintillator	LSO	LYSO	LBS
Crystal size (mm)	4 × 4 × 20	4 × 4 × 22	4 × 5.3 × 25
Crystal number	28,672	28,336	20,160
Photodetector	APD	PMT	SiPM
TOF	No	Yes	Yes
Energy resolution (%)	14.5	12	10.5
Energy window (keV)	430–610	460–665	425–650
Time resolution (ns)	2.93	0.53	0.39
Coincidence window (ns)	5.86	6.00	4.57
Transaxial FOV (cm)	59.4 cm	//	60 cm
Axial FOV	25.8 cm	18	25 cm
Sensitivity (kcps/MBq)	15.0	7.0	22.2
Scatter fraction (%)	37.9	26.0	43.4
Peak NECR (kcps @ kBq/mL)	184@ 23.1	88.5@13.7	218@17.7
MR			
Field strength (T)	3	3	3
Bore (cm)	60	60	60
FOV (cm^3)	50 × 50 × 50	50 × 50 × 45	50 × 50 × 50
Gradient mT/m	45	40	44
Slew rate (T/m)/s	200	100	200

respectively, the attenuation correction factor obtained from CT must be scaled to the 511 keV photons applying a scaling factor defined by the ratio of the μ of the 511 keV photons to that of the 70 keV X-rays in a given tissue [1].

PET/MRI is a multi-modality technology combining the functional information of PET with the soft-tissue contrast of MRI. Actually, two approaches are implemented in the commercial PET/MRI scanners: sequential PET/MRI [7–9]. The characteristics of the three commercial PET/MRI scanners are summarized in Table 1.3.

1.3 Positron Emission Tomography Radiopharmaceuticals

Radiopharmaceuticals are radiolabelled molecules consisting in a molecular structure and a radioactive nuclide. The first one defines the pharmacokinetics and dynamics within the organism, while the latter is responsible for a detectable signal and for the consequent image visualization [10]. To maintain the stability of these two components, a linker may be necessary. The most important PET nuclides and their physical characteristics are summarized below:

- Carbon-11 (^{11}C) has a physical half-life of about 20 min and decays by β^+ emission (99.75%) and by electron capture (0.25%) to the ground state of the stable nuclide Boron-11 (^{11}B). β^+ average energy is 386 keV, corresponding to a mean range in water of 1.3 mm. ^{11}C can be produced by different nuclear reactions; however, the main production mode is targeting Nitrogen-14 (^{14}N) with cyclotron accelerated protons: $^{14}N(p,\alpha)^{14}C$.
- Fluorine-18 (^{18}F) has a physical half-life of about 110 min and decays by β^+ emission (96.86%) and electron capture (3.14%) directly to the ground state of the stable

nuclide Oxygen-18 (^{18}O). β^+ average energy is 250 keV, corresponding to a mean range in water of 0.6 mm. ^{18}F can be produced by different nuclear reactions; however, the main production mode is targeting Oxygen-18 with cyclotron accelerated protons: ^{18}O(p,n)^{18}F.

- Gallium-68 (^{68}Ga) has a physical half-life of about 67.8 min and decays by β^+ emission (88.88%) and by electron capture (11.11%) into ^{68}Zn. β^+ average energy is 830 keV, corresponding to a mean range in water of 3.6 mm. ^{18}Ga can be produced by different nuclear reactions; however, the main production mode is using a Germanium-68 (^{68}Ge)-^{68}Ga generator.
- Iodine-124 (^{124}I) has a physical half-life of about 4.2 days and decays by β^+ emission (23%) and by electron capture (77%) to the excited level and the ground state of Tellurium-124 (^{124}Te). β^+ average energy is 836 keV, corresponding to a mean range in water of 3.4 mm. ^{124}I can be produced by different nuclear reactions; however, ^{124}Te(p,n) reaction gives the purest form of ^{124}I.
- Copper-64 (^{64}Cu) has a physical half-life of about 12.7 h and decays by β^- emission (38%) to Zinc-64 (^{64}Zn) and by β^+ emission (17.4%) or electron capture (44.6%) to the excited level and the ground state of Nickel-64 (^{64}Ni). β^+ average energy is 278 keV, corresponding to a mean range in water of 0.7 mm. The main ^{64}Cu production modes are the following: ^{63}Cu(n,γ)^{64}Cu, ^{65}Cu(n,2n)^{64}Cu, ^{64}Zn(n,p)^{64}Cu, ^{64}Zn (d,2p)^{64}Cu.

The wide and feasible availability of positron emitters radionuclides is a prerequisite for successful application on a routine basis. Fluorine-18 and Gallium-68 are the most used in a clinical setting, so far. Due to its versatility, ^{18}F-Fluorodeoxyglucose (FDG), namely a radiolabelled analogue of glucose, is the by far most widely used PET radiopharmaceutical worldwide. FDG is very useful to detect malignant tumours characterized by increased glucose metabolism. However, FDG remains a non-specific tracer and its uptake is also been observed in many benign conditions, such as infective and inflammatory processes. Therefore, over the last decade, there is a growing interest in researching and using new radiopharmaceuticals, such as radiolabelled amino acids, nucleoside derivatives, choline derivatives, nitroimidazole derivatives and peptides, able to carefully target specific biomarkers. These new generation radiopharmaceuticals allow the analysis of several molecular pathways in tumour biology including metabolism, proliferation, oxygen delivery and protein synthesis as well as receptor and gene expression (Tables 1.4, 1.5 and 1.6). Some examples of PET images with different radiopharmaceuticals are showed in Figs. 1.1 and 1.2.

Table 1.4 Metabolic and pure isotope PET tracers

Metabolic tracers	Clinical indication in oncology	Uptake mechanism	Physiological biodistribution	Patient preparation	Time from injection to acquisition	Recommended activity in adults	Paediatric recommended activity	Effective dose for adults (mSv/MBq)
^{18}F-FDG	– Differentiation of benign from malignant lesions – Searching for an unknown primary tumour – Staging patients with known malignancies – Monitoring the effect of therapy – Detecting tumour recurrence – Guiding biopsy – Guiding radiation therapy planning	Depends on the expression of GLUT1 transport and hexokinase phosphorylation.	*Intense uptake*: grey matter, myocardium, urinary tracts, bladder *Mild uptake* Liver, spleen, bowel and bone marrow	Fasting (4 h) No physical activity (1 day) Empty bladder	60 min	Dependent on the system, time per bed position and the patient's weight	3.7–5.2 MBq/kg for a body PET/CT scan	1.9E − 02
^{18}F-Choline	– Detecting prostate cancer recurrence – Staging of high-risk prostate cancer – Monitoring the effect of therapy in advanced or castration-resistant prostate cancer	Depends on the expression of choline transporters and choline kinase activity.	*Intense uptake* Salivary glands, liver, pancreas, spleen, kidney, urinary tracts, bladder *Mild uptake* Lacrimal glands, bowel and bone marrow	Fasting (4 h) No physical activity (1 day) Empty bladder	Dual phase procedure: a static acquisition of the pelvis immediately after injection followed by a whole body scan 60 min after injection	3–4 MBq/kg	Not applicable	3.0E − 2

(continued)

Table 1.4 (continued)

^{11}C-Choline	– Detecting prostate cancer recurrence – Staging of high-risk prostate cancer – Monitoring the effect of therapy in advanced or castration-resistant prostate cancer	Depends on the expression of choline transporters and choline kinase activity	*Intense uptake* Salivary glands, liver, pancreas, spleen, kidney *Mild uptake* Lacrimal glands, bowel and bone marrow	Fasting (6 h) Empty bladder	0–15 min	370 MBq	Not applicable	4.9E − 3
^{18}F-Fluociclovine	Detecting early prostate cancer recurrence	Depend on the expression of l-type amino acid transporter–alanine-serine-cysteine transporter 2 *(LAT/ASCT2)*	*Intense uptake* Liver and pancreas *Mild uptake* Lacrimal glands, salivary gland, bowel and bone marrow	Fasting (4 h) No physical activity (1 day) Empty bladder	3–5 min	370 MBq	Not applicable	2.2E − 2
^{18}F-DOPA	– Detection of insulinomas, paragangliomas and pheochromocytoma – Detecting medullary thyroid cancer recurrence – Staging of medullary thyroid cancer – Staging and restaging of neuroblastoma	Depends on the expression of large neutral amino acid transporter (LAT)	*Intense uptake* basal ganglia, pancreas, gallbladder, kidney and bladder *Mild uptake* Salivary gland, liver, bowel and bone marrow	Fasting (4 h) Empty bladder	10–60 min	2–4 MBq/kg	4 MBq/kg	2.5E − 02

Pure isotopes as PET tracers	Clinical indications in oncology	Uptake mechanism	Physiological biodistribution	Patient preparation	Time from injection to acquisition	Recommended activity in adults	Paediatric recommended activity	Effective dose for adults (mSv/MBq)
^{18}F-NaF	Detection of bone metastases	Chemisorption of fluoride ions onto the surface of hydroxyapatite depending on bone blood flow and osteoblastic activity	Uniform tracer distribution throughout the skeleton	Empty bladder	30–45 min	1.5–3.7 MBq/kg	2.2 MBq/kg	2.4E − 2
^{124}I-NaI	– Detect differentiated thyroid cancer (DTC) recurrence – Select patients for further radioiodine treatment – Dosimetric studies for radioiodine treatment	Depends on sodium/iodide symporter (NIS) expression	*Intense uptake* Salivary glands, oral cavity, gastrointestinal tract, bladder	Injection of recombinant human TSH or 2–4 weeks of thyroid hormone withdrawal	24,72, 96 h	24–80 MBq	22–60 MBq	9.5E − 2 (for 0% thyroid uptake)
$^{64}CuCl_2$	Detecting early prostate cancer recurrence	Depends on human copper transport 1 (HCTR1)	High uptake in the liver and less intense uptake in salivary glands, biliary tract, pancreas, spleen and kidney	Fasting (4 h)	1 h	250 MBq	Not applicable	2.9E − 2

Table 1.5 Receptor PET tracers

Receptor tracers	Indications (oncology)	Uptake mechanism	Physiological biodistribution	Patient preparation	Time from injection to acquisition	Recommended activity in adults	Paediatric recommended activity	Effective dose for adults (mSv/MBq)
^{68}Ga-DOTA-conjugated peptides	– Localization of neuroendocrine tumours and detection of metastatic disease (staging) – Monitoring the effect of therapy in these patients – Select patients with metastatic disease for somatostatin receptor radionuclide therapy	Depends on the expression of somatostatin receptors (SSTR)	*Intense uptake* Liver, spleen, kidney, bladder *Moderate uptake* Pituitary gland, salivary glands	No need for fasting before injection No consensus on discontinuation of cold octreotide therapy	60 min	100–200 MBq	In neuroblastoma proposed 2.6 MBq/kg	2.2E − 2
^{64}Cu-DOTA-conjugated peptides	– Localization of neuroendocrine tumours and detection of metastatic disease (staging) – Monitoring the effect of therapy in these patients – Select patients with metastatic disease for somatostatin receptor radionuclide therapy	Depends on the expression of somatostatin receptors (SSTR)	*Intense uptake* Liver, spleen, kidney, bladder *Moderate uptake* Pituitary gland, salivary glands, bowel	No need for fasting before injection No consensus on discontinuation of cold octreotide therapy	60 min	200 MBq	Not applicable	3.2E − 2
^{68}Ga-PSMA	– Detecting prostate cancer recurrence – Staging of high-risk prostate cancer – Monitoring of systemic treatment in metastatic prostate cancer	Depends on increased PSMA expression	*Intense uptake* Salivary glands, kidney, bladder, liver, spleen, bowel	Patients do not need to fast and are allowed to take all their medications	60 min	1.8–2.2/kg	Not applicable	2.0E − 2

^{18}F-PSMA	– Detecting prostate cancer recurrence – Staging of high-risk prostate cancer – Monitoring of systemic treatment in metastatic prostate cancer	Depends on increased PSMA expression	*Intense uptake* Salivary glands, kidney, bladder, liver, spleen, bowel	Patients do not need to fast and are allowed to take all their medications.	90 min	350 MBq	Not applicable	1.3E − 2
^{64}Cu-PSMA	– Detecting prostate cancer recurrence	Depends on increased PSMA expression	*Intense uptake* Salivary glands, kidney, bladder, liver, spleen, bowel	Patients do not need to fast and are allowed to take all their medications	60 min	315 MBq	Not applicable	2.5E − 2
^{18}F-FES	– Detecting disease relapse in breast cancer patients with high levels of oestrogen receptors – Predicting response to endocrine treatment in metastatic breast cancer patients	Depends on the expression of oestrogen receptors	*Intense uptake* Liver, bile duct, intestinal tract and bladder	– Discontinuation of oestrogens receptor antagonist fo 5 days. Aromatase inhibitors are allowed – Premenopausal patients might have impaired uptake of ^{18}F-FES because of competitive binding by endogenous oestrogens	60 min	200 MBq	Not applicable	2.2E − 2

Table 1.6 Brain PET tracers

Brain tracers	Clinical indications	Uptake mechanism	Biodistribution	Patient preparation	Waiting time from radiopharmaceutical administration	Recommended activity in adults	Paediatric recommended activity	Effective dose per administration activity for adults (mSv/MBq)
^{18}F-FDG	*Neurology* – Early and differential diagnosis of dementia – Epilepsy – Differentiation between Parkinson's disease and atypical parkinsonian syndromes *Neurooncology* – Differential diagnosis of cerebral lesions, detection of viable tumour tissue and for grading	Depends on the expression of GLUT1 transport and hexokinase phosphorylation	*Intense uptake* Grey matter	– Fasting (4 h) – Empty bladder – Centrally acting pharmaceuticals should be discontinued on the day of the PET scan according to the clinical status of the patient	30–60 min	150–250 MBq	0.1 mCi/kg	1.9E − 02
^{18}F-DOPA	*Neurology* – To differentiate essential tremor from parkinsonian syndromes – Differentiation between Lewy body disease and other dementias – To differentiate degenerative from non-degenerative parkinsonism – To detect early presynaptic parkinsonian syndromes *Neurooncology (glioma)* – Differentiation of grade III and IV gliomas from nonneoplastic lesions or grade I and II gliomas – Prognostication of gliomas – Definition of the optimal biopsy site – Diagnosis of tumour recurrence – Disease and therapy monitoring	– Depends on the activity of enzyme aromatic amino acid decarboxylase converting 6-^{18}F-L-dopa in fluorodopamine – Depends on the expression of large neutral amino acid transporter (LAT)	*Intense uptake* Basal ganglia *Low-moderate uptake* Grey matter	– Fasting (4 h) – Empty bladder – Premedication with carbidopa (2 mg/kg) 1 h before the injection	*Neurology* 70–90 min *Neurooncology* 10–30 min	185 MBq	74–111 MBq	2.5E − 02

^{18}F-FET	*Neurooncology (glioma)* – Differentiation of grade III and IV tumours from nonneoplastic lesions or grade I and II gliomas – Prognostication of gliomas – Definition of the optimal biopsy site – Diagnosis of tumour recurrence – Disease and therapy monitoring	Depends on the expression of large neutral amino acid transporter (LAT)	*Low uptake* Grey matter	Fasting (4 h) – Empty bladder	20 min	185 MBq	100 MBq	1.6E − 2
^{11}C-MET	*Neurooncology (glioma)* See ^{18}F-FET	Depends on the expression of large neutral amino acid transporter (LAT)	*Low uptake* Grey matter	Fasting (4 h) – Empty bladder	10 min	370 MBq	11 MBq/kg	5.0E − 03
^{18}F-Flutemetamol	Patients with a diagnosis of possible Alzheimer disease or mild cognitive impairment when the diagnosis is uncertain after morphological the and functional neuroimaging	High affinity amyloid-beta neuritic plaques	*Low uptake* White matter	– Empty bladder	90 min	185 MBq	Not applicable	3.5E − 2
^{18}F-Florbetaben	Patients with a diagnosis of possible Alzheimer disease or mild cognitive impairment when the diagnosis is uncertain after morphological the and functional neuroimaging	High affinity amyloid-beta neuritic plaques	*Low uptake* White matter	– Empty bladder	90 min	300 MBq	Not applicable	1.9E − 2

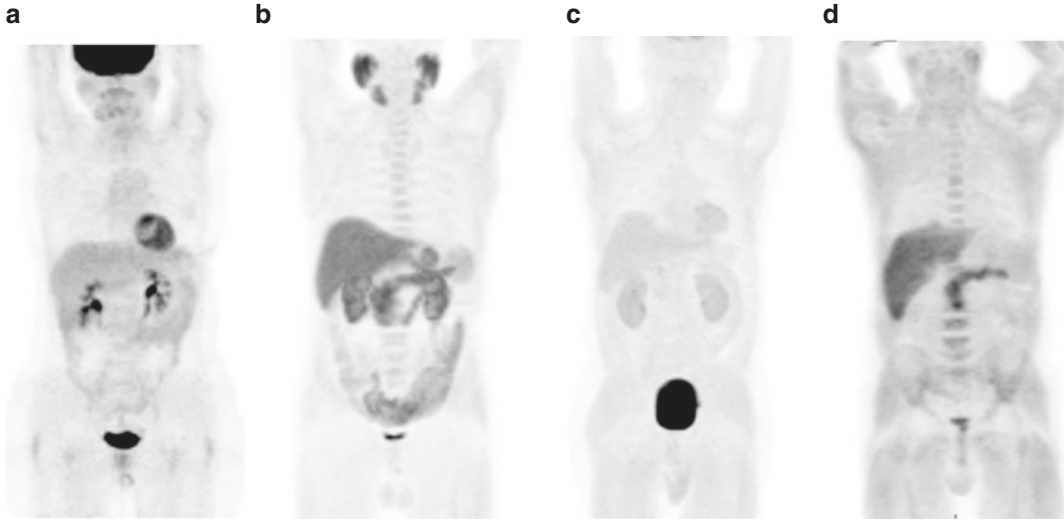

Fig. 1.1 Biodistribution of PET tracers: ^{18}F-FDG (**a**), ^{18}F-FCH (**b**), ^{18}F-DOPA (**c**), ^{18}F-Fluociclovine (**d**)

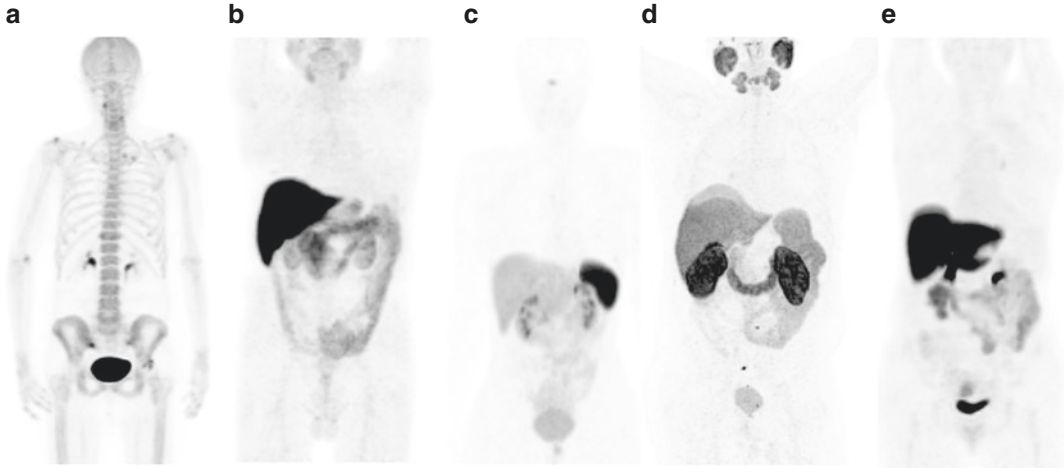

Fig. 1.2 Biodistribution of PET tracers: ^{18}F-NaF (**a**), $^{64}CuCl_2$ (**b**) ^{68}Ga-DOTATOC (**c**), ^{68}Ga-PSMA (**d**), ^{18}F-FES (**e**)

References

1. Saha GB. Basics of PET imaging: physics, chemistry, and regulations. New York: Springer; 2010.
2. Zanzonico P. Positron emission tomography: a review of basic principles, scanner design and performance, and current systems. Semin Nucl Med. 2004;34(2):87–111.
3. Slomka PJ, Pan T, Germano G. Recent advances and future progress in PET instrumentation. Semin Nucl Med. 2016;46(1):5–19.
4. Alessio A, Kinahan P. PET imaging reconstruction http://faculty.washington.edu/aalessio/papers/alessio-PETRecon.pdf.
5. Waterstram-Rich KE, Christian PE. Nuclear medicine and PET/CT: technology and techniques. St. Louis: Elsevier Mosby; 2012.
6. Li S, Tavares JMRS. Shape analysis in medical image analysis, 51. Lecture notes in computational vision and biomechanics, vol. 14; 2014.
7. Zaidi H, Ojha N, Griesmer J, et al. Design and performance evaluation of a whole-body ingenuity TF PET–MRI system. Phys Med Biol. 2011;56(10):3091–106.

8. Delso G, Furst S, Jakoby B, et al. Performance measurements of the Siemens mMR integrated whole-body PET/MR scanner. J Nucl Med. 2011;52(12):1914–22.
9. Grant AM, Deller TW, Khalighi MM, et al. NEMA NU 2-2012 performance studies for the SiPM-based ToF-PET component of the GE SIGNA PET/MR system. Med Phys. 2016;43(5):2334.
10. Wadsak W, Mitterhauser M. Basics and principles of radiopharmaceuticals for PET/CT. Eur J Radiol. 2010;73:461–9.